HHS Public Access

Author manuscript

Arch Biochem Biophys. Author manuscript; available in PMC 2018 January 01.

Published in final edited form as:

Arch Biochem Biophys. 2017 January 01; 613: 12–22. doi:10.1016/j.abb.2016.10.016.

Reciprocal regulation of acetyl-CoA carboxylase 1 and senescence in human fibroblasts involves oxidant mediated p38 MAPK activation

Inés Marmisolle[a], **Jennyfer Martínez**[a], **Jie Liu**[b], **Mauricio Mastrogiovanni**[a], **María M. Fergusson**[b], **Ilsa I. Rovira**[b], **Laura Castro**[a], **Andrés Trostchansky**[a], **María Moreno**[c], **Liu Cao**[b,1], **Toren Finkel**[b,*], and **Celia Quijano**[a,*]

[a]Center for Free Radical and Biomedical Research and Departamento de Bioquímica, Facultad de Medicina, Universidad de la República, Montevideo, Uruguay.

[b]Center for Molecular Medicine, National Heart, Lung and Blood Institute, National Institutes of Health, Bethesda, MD.

[c]Laboratory for Vaccine Research, Departamento de Desarrollo Biotecnológico, Facultad de Medicina, Instituto de Higiene, Universidad de la República.

Abstract

We sought to explore the fate of the fatty acid synthesis pathway in human fibroblasts exposed to DNA damaging agents capable of inducing senescence, a state of irreversible growth arrest. Induction of premature senescence by doxorubicin or hydrogen peroxide led to a decrease in protein and mRNA levels of acetyl-CoA carboxylase 1 (ACC1), the enzyme that catalyzes the rate-limiting step in fatty-acid biosynthesis. ACC1 decay accompanied the activation of the DNA damage response (DDR), and resulted in decreased lipid synthesis. A reduction in protein and mRNA levels of ACC1 and in lipid synthesis was also observed in human primary fibroblasts that underwent replicative senescence.

We also explored the consequences of inhibiting fatty acid synthesis in proliferating non-transformed cells. Using shRNA technology, we knocked down ACC1 in human fibroblasts.

* Correspondence should be addressed to: Celia Quijano, Center for Free Radical and Biomedical Research and Departamento de Bioquímica, Facultad de Medicina, Universidad de la República, Montevideo, Uruguay 11800; Telephone: +598-2-924 3414 ext. 3401; celiq@fmed.edu.uy or Toren Finkel, Center for Molecular Medicine, National Heart, Lung and Blood Institute, National Institutes of Health, Bethesda, MD, USA, 20892; Telephone: +1-301-402-4081, finkelt@nhlbi.nih.gov.

[1]Present address: Key Laboratory of Medical Cell Biology, Ministry of Education, China Medical University, Shenyang, China.

Author contribution statement

CQ, TF and LCao conceived and designed the experiments. IM performed and analyzed most of the experiments shown in Figures 1 to 3 and S1. CQ performed and analyzed most of the experiments in Figures 4 to 6 and S2- S4. JL and LCastro performed and analyzed experiments involving oxidant formation. JM and MMoreno designed and performed the RT-qPCR experiments for ACC1. MMF designed and performed the RT-qPCR experiments for FAS. IR provided technical assistance and contributed to the preparation of the figures. MMastrogiovanni and AT collaborated in the design and execution of lipid synthesis assays. CQ wrote the manuscript and all authors reviewed the results and approved the final version of the manuscript.

Declaration of interest

The authors declare that they have no conflicts of interest with the contents of this article.

Interestingly, this metabolic perturbation was sufficient to arrest proliferation and trigger the appearance of several markers of the DDR and increase senescence associated β-galactosidase activity. Reactive oxygen species and p38 mitogen activated protein kinase phosphorylation participated in the induction of senescence. Similar results were obtained upon silencing of fatty acid synthase (FAS) expression. Together our results point towards a tight coordination of fatty acid synthesis and cell proliferation in human fibroblasts.

Graphical Abstract

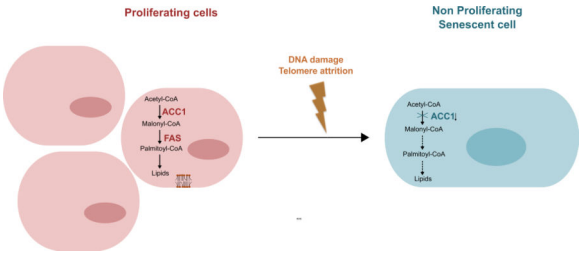

Keywords

Lipid synthesis; acetyl-CoA carboxylase 1; cellular senescence; DNA damage response; reactive oxygen species (ROS); p38 MAPK

1. Introduction

Cellular senescence is a state of irreversible growth arrest that can be triggered by a variety of stimuli in both physiological and pathological situations [1]. In addition to the lack of proliferation, senescent cells exhibit characteristic morphological changes, senescence-associated β-galactosidase expression (SA-β-Gal) due to an increase in lysosomal content, activation of the DNA damage response (DDR), heterochromatic foci and a secretory phenotype [1, 2].

Several stimuli can induce senescence, including telomere attrition (replicative senescence), DNA damage, strong mitogenic signals produced by oncogenes and epigenetic perturbations [2]. These stimuli trigger the DDR through the activation of the protein kinase ataxia-telangiectasia mutated (ATM) [3], leading to the formation of nuclear foci with DNA repair proteins and phosphorylated histone H2AX (γ-H2AX), phosphorylation and stabilization of p53 and increased transcription of p21 [3]. Stimuli that produce a DDR can also increase p16 expression, through derepression of the cyclin dependent kinase inhibitor 2A (CDKN2A) locus [1]. The cyclin-dependent kinase (Cdk) inhibitors p21 and p16 maintain the Retinoblastoma protein (pRb) in a hypophosphorylated and active state, preventing cell cycle progression [3]. Reactive oxygen species (ROS) are augmented in senescence and contribute to the establishment and maintenance of the senescent state. Mechanistically ROS have been implied in persistent DDR signaling [4] and activation of the p38 mitogen activated protein kinase (p38 MAPK); inducing proliferation arrests both in ATM dependent and independent fashion [5, 6].

Senescence induction is also accompanied by profound changes in metabolic programs that adapt to the requirements of the new phenotype [7], were growth arrest is probably a relevant determinant. Cell proliferation and metabolic pathways are tightly linked in mammalian cells and proliferating cells are characterized by high rates of macromolecule biosynthesis, such as fatty acids [8]. Pharmacological inhibition or knockdown of enzymes involved in fatty acid synthesis promotes growth arrest, apoptosis and increased autophagy in cancer cells [9]. While the fatty acid synthesis pathway has been extensively explored in cancer cells, not much is known about the fate of this anabolic pathway in senescent cells.

The initial steps in the biosynthesis of fatty acids are accomplished by acetyl-CoA carboxylase (ACC) that catalyzes the ATP dependent carboxylation of acetyl-CoA to malonyl-CoA; and fatty acid synthase (FAS) that catalyzes the condensation reactions leading to the synthesis of palmitate. In human tissues, two ACC isoforms have been described [10]: ACC1 which catalyzes a committed and rate-limiting step in the biosynthesis of long chain fatty-acids, and ACC2 that participates in the regulation of mitochondrial fatty acid oxidation [11]. Recent reports indicate that the enzymatic activity and expression of ACC1 is regulated in coordination with cell proliferation. ACC1 binding to the tumor suppressor BRCA1 modulates its activity in a cell cycle dependent manner [12] and cyclin D1 inhibits ACC1 gene expression [13].

We have observed that fatty acid synthesis is inhibited in fibroblasts undergoing oncogene-induced senescence. [14]. While conflicting reports regarding fatty acid synthesis can be found in replicative senescence, were both a decrease and an increase in fatty acid synthesis enzymes has been observed [15, 16].

Here we explore the activity of the fatty acid synthesis pathway after the exposure to DNA damaging agents capable of inducing premature senescence and in replicative senescent fibroblasts. We measure the levels and expression of ACC1 and endogenous lipid synthesis in fibroblasts as they enter a proliferation arrest. In addition, we assess the impact of inhibiting lipid synthesis on proliferating human fibroblast, targeting ACC1 and FAS with both shRNA and pharmacological inhibitors.

2. Materials And Methods

2.1. Cell culture

IMR-90 (ATCC® CCL-186) human lung fibroblasts were obtained from ATCC (Manassas, Virginia, USA) and used after 10 passages in culture and at a population doubling level (PDL) of 25. Cells were subcultured weekly using an initial seeding density of 0.5×10^6 cells per 10 cm dish. IMR-90 cells were routinely grown in Dulbecco's modified Eagle's medium (DMEM, Invitrogen) supplemented with 10% (v/v) fetal bovine serum (FBS), penicillin 50 U/ml and streptomycin 50 μg/ml. Cells were maintained at 37°C in a CO_2 incubator (95% air, 5% CO_2). Under our experimental conditions, IMR-90 cultures entered senescence after achieving a PDL value of 50 obtained after 22-24 passages. At this point, fibroblasts could not reach confluence after 7-10 days following a 1:2 split and 60-80% cells stained positive for SA-β-Gal. Cells between passage 10-18 were denominated early passage cells (PDL 25-36), while those between 19 -23 (PDL 39-47) were considered mid-passage cells.

2.2. Pharmacological treatments

For doxorubicin (Sigma) treatment cells were seeded at 1-4 $\times 10^4$ cell/cm^2, 2-3 days after plating cells were incubated with 0.2 μM doxorubicin, for the indicated periods.

Hydrogen peroxide (H_2O_2) was quantified spectrophotometrically (ε_{240} = 43.6 M^{-1} cm^{-1}) and treatment was performed as described [17]. Briefly, cells were seeded at 1-4 $\times 10^4$ cell/cm^2 and twenty-four hours later exposed for two hours to 600 μM H_2O_2 in complete media. Four days after the first treatment the cells were split 1:3 and the next day were treated again for two hours with 600 μM H_2O_2.

For pharmacological inhibition of fatty acid synthesis, subconfluent early passage cells were incubated for 5 days with the FAS inhibitor tetrahydro-4-methylene-2R-octyl-5-oxo-3S-furancarboxylic acid (C75) or the ACC1 inhibitor 5-(tetradecyloxy)-2-furancarboxylic acid (TOFA). The media containing the drugs was changed every two days.

2.3. Lentiviral shRNA transduction

Lentiviral short hairpin RNA (shRNA) constructs were purchased from Open Biosystems (shACC1: ID TRCN0000029027; shACC1_#2: TRCN0000029025 plus TRCN0000004767, Control: pLKO.1 empty vector control plasmid) or Sigma-Aldrich (shFAS: ID TRCN0000003125; shFAS_#2: TRCN0000003127; non-target shRNA: SHC002) [48]. Plasmids carrying VSVG envelope protein (pCMV-VSV-G was a gift from Bob Weinberg, Addgene plasmid # 8454) and packaging plasmid (pCMV-dR8.2 dvpr was a gift from Bob Weinberg, Addgene plasmid # 8455) for lentiviral constructs were obtained from Addgene [48]. Lentiviral vectors were produced in 293T cells according to protocols established by the Broad Institute RNAi Consortium (http://www.broadinstitute.org/genome_bio/trc/publicProtocols.html). One to two days after seeding, early passage IMR-90 cells were transduced with lentiviruses (MOI of 1-5) overnight in media with 8 μg/ml polybrene. Infected cells were subsequently selected in culture media supplemented with 2 μg/ml puromycin (Sigma-Aldrich). Experiments were performed four to six days after infection, unless otherwise specified.

2.4. Lipid Synthesis

Lipid biosynthesis was assessed as previously described using the incorporation of [^{14}C]-acetate into cell lipids [18]. IMR-90 cells were seeded onto 6 cm dishes and on the day of the experiment, cells were washed with PBS and then incubated for two hours in 2 ml of DMEM supplemented with 4.5 g/l D-glucose and 0.1% FBS. Acetic Acid [2-^{14}C] sodium salt (2 μCi, Perkin Elmer) was added to the cells for a three hour pulse, after which the cells were washed with PBS, harvested, centrifuged and washed again with PBS. Organic extraction of the cell lipids was performed as previously described by Bligh and Dyer [19]. Radioactivity was determined in the incubation media, aqueous phase and organic phase using a liquid scintillation counter. Radioactivity in the organic phase was normalized to protein content.

2.5. SA-β-Gal activity

For senescence-associated β-galactosidase (SA-β-Gal) assay, cells were washed twice in PBS, fixed for five minutes in 2% formaldehyde, 0.2% glutaraldehyde in PBS, washed three times in PBS, and incubated at 37°C overnight in fresh SA-β-Gal staining solution at pH 6 as previously described [20]. Percentage positive staining was calculated by counting under the microscope at least one hundred cell in five different fields.

2.6. γ-H2AX foci

IMR-90 fibroblasts were cultured on chamber slides that were first fixed with 4% paraformaldehyde in PBS for ten minutes and then permeabilized for an additional ten minutes with 0.2% Triton X-100 in PBS. After permeabilization, cells were incubated for one hour in blocking buffer composed of 0.2% Triton X-100 and 3% BSA in PBS and then with primary antibody anti γ-H2AX (Ser139) (Millipore #07-164, 1:2000) overnight at 4°C. The following day, slides were incubated with a rhodamine (TRITC) conjugated Goat Anti-Rabbit IgG secondary antibody (Jackson Immunoresearch). DAPI (4', 6-diamidino-2-phenylindole) was used to stain the nucleus. The percentage of cells with foci formation in their nuclei were determined after counting more than one hundred random cells in five different fields.

2.7. Protein levels and phosphorylation assays

Cells were routinely lysed in cell lysis buffer containing 20 mM Tris, pH 7.4, 1 % Triton X-100, 20 mM Tris-HCl (pH 7.5), 150 mM NaCl, 1 mM EDTA, 1 mM EGTA, 2.5 mM sodium pyrophosphate, 1 mM β-glycerophosphate, 1 mM Na_2VO_4, supplemented with protease and phosphatase inhibitor cocktails. Lysates were sonicated, centrifuged at 14000 g for ten minutes and stored at −80°C. Proteins (20-40 μg) were resolved by SDS-PAGE and subjected to Western blotting using standard procedures. The following primary antibodies were used: ACC (#3676, 1:1000), FAS (#3180, 1:1000), phospho-p53 (Ser15) (#9284, 1:1000), p21 (#2947), p38 MAPK (#9228, 1:1000), phospho-p38 MAPK (Thr180/Tyr182) (#9215, 1:1000) and GAPDH (#2118, 1:1000) were from Cell Signaling Tech; phospho-ATM (Ser1981) (#05-740, 1:1000) was from Millipore; phospho-pRb (Ser807/Ser811) (#558389, 1:10000) from BD Pharmingen; phospho-H2AX (Ser139) was from Novus (NB-384, 1:1000), p53 (DO-1, sc-126, 1:250) and α-tubulin (sc-8035, 1:500) from Santa Cruz Biotechnology. Western Blots were analyzed with Image Studio Lite (LI-COR Bioscience).

2.8. ACC1 gene expression analysis

For ACC1 gene expression analysis, total cellular RNA from IMR-90 fibroblasts was extracted with TRIzol Reagent (Life Technologies). RNA quality and quantity was assessed by spectrophotometric measurements at 260/280 nm using a NanoDrop 2000 (Thermo Scientific) after extraction. Prior to cDNA synthesis, 1 μg of total RNA was treated with DNAse-I (Invitrogen) according to the manufacturer's instructions. Retrotranscription was performed in a final volume of 20 μl in the presence of random primers (200 ng), dNTPs (0.5 mM), DTT (0.01 M), RNaseOUT (40 U) and M-MLV Reverse Transcriptase (Invitrogen). Quantitative RT-PCRs for *Actb* and *Acc1* mRNA levels were conducted using

QuantiTect® SYBR® Green PCR Kit (Qiagen) in a Rotor-Gene 6000 (Corbett) and the following primers (forward and reverse respectively):

ACC1: 5'-ATTGGGGCTTACCTTGTCCG-3' and 5'-CGAGGACTTTGTTGAGGGCT-3'

Actin: 5'-CTACGAGCTGCCTGACGG-3' and 5'-AGGACTCCATGCCCAGGAA-3'

Beta-Actin encoding gene *Actb* was used as house-keeping gene. The relative mRNA amount in each sample was calculated using the $2^{-\Delta\Delta Ct}$ method [21] where $\Delta Ct = Ct_{Acc1} - Ct_{Actb}$, and expressed as relative mRNA levels in treated compared to untreated cells.

2.9. FAS gene expression analysis

For FAS gene expression analysis, total cellular RNA from IMR-90 fibroblasts was extracted with the NucleoSpin RNA II RNA isolation kit (Macherey-Nagel) and then reverse-transcribed into complementary DNA (cDNA) with the SuperScript III First-Strand Synthesis SuperMix for qRT-PCR (Invitrogen). PCRs were set up with the Power SYBR Green PCR Master Mix (Applied Biosystems). Primers (forward and reverse respectively) used included:

FAS: 5'-CGACAGCACCAGCTTCGCCA-3' and 5'-CTCCGCAAGCACCTGCACGA-3'.

Actin: 5'-TGAGAGGGAAATCGTGCGTGAC-3' and 5'-AAGAAGGAAGGCTGGAAA AGAG-3'

The relative mRNA amount in each sample was calculated as described for ACC1 gene expression.

2.10. Growth curves and population doubling

Cells were seeded in 12-well plates, detached at the indicated times using Tryple express and the number of live cells was determined by dye exclusion of Trypan blue (Invitrogen) in a Countess Automated Cell Counter (Invitrogen). The population doublings (PD) were calculated by the formula:

$$[log10\,(N_{\mathrm{H}}) - log10\,(N_{\mathrm{I}})]\,/Log10\,(2) = X$$

Where N_I = inoculum number, N_H = cell harvest number, and X = PD. The calculated PD is then added to the previous population doubling level to yield the cumulative population doubling (cPDL) [22].

2.11. Cell proliferation

Cell proliferation was measured assessing the incorporation of the thymidine analogue bromodeoxyuridine (BrdU, BD Pharmingen) to DNA. IMR-90 fibroblasts were cultured on permanox chamber slides (Nunc), incubated with 10 μM BrdU, for twenty-four or forty-eight hours, fixed with cold EtOH 80% overnight at −20°C and washed with PBS. The slides were treated with HCl 2 N in PBS for 30 min and washed with PBS to neutralize HCl. Cells

were washed, blocked in Tween 0.1% BSA 1% in PBS and an anti-BrdU antibody conjugated with FITC (Becton Dickinson) used for staining. Cells were mounted with Vectashield mounting media for fluorescence with DAPI (Vector Laboratories Inc.). The percentage positive staining was calculated by counting BrdU stained nuclei in more than one hundred random cells in five different fields.

Alternatively, [methyl ^{3}H]-thymidine incorporation into DNA was assessed as previously described [23]. Briefly, one μCurie of [methyl-^{3}H] thymidine (Perkin Elmer) was added for twenty-four hours to the culture media of cells in 6 cm dishes. Cells were harvested and a small aliquot reserved for cell protein measurements using the Bicinchoninic acid technique (Pierce). DNA was extracted by precipitation with TCA (20% w/v in water) at 4°C, consecutively washed with 10% TCA and 95% ethanol, dried and solubilized in 0.5N NaOH/ 0.5% SDS. Radioactivity was determined with a liquid scintillation counter and normalized by cell protein. Results are expressed as a percentage of [methyl ^{3}H]-thymidine incorporation per mg of protein in control cells.

2.12. Intracellular reactive oxygen species

Intracellular reactive oxygen species **(**ROS) were measured after the incubation with 5 μM 5-(and-6)-chloromethyl-2′,7′-dichlorodihydrofluorescein diacetate, (CM-DCFHDA, Invitrogen) in PBS for thirty minutes at 37°C, followed immediately by flow cytometry analysis using a FACSCanto instrument (BD Bioscience). The 2'-7'-dichlorodihydrofluorescein (DCFH) moiety can react with several one electron-oxidant species (e.g. hydroxyl radical, carbonate radical, nitrogen dioxide, alkyl radical) leading to the formation of the fluorescent compound 2'-7'-dichlorofluorescein (DCF). It is a sensitive, yet non- specific probe for ROS [24]. Viable cells, as determined by 7-AAD (Invitrogen) staining, were used for the analysis of ROS levels. Where indicated, cells were treated with freshly prepared 0.75 mM N-acetylcysteine (Sigma) in culture media before assessment of ROS levels.

2.13. Statistical analysis

Data was statistically analyzed by unpaired Student's t test; two tailed p values are reported. Results are reported as the mean ± standard error (SEM).

3. Results

3.1. Down-regulation of ACC1 and inhibition of lipid synthesis in human primary fibroblasts exposed to DNA damaging agents

Coordination between cell proliferation and anabolism has been extensively studied in cancer cells, and an increase in biosynthetic pathways appears as a hallmark of malignant transformation [8, 9]. Yet few studies have explored these events in non-malignant cells. Since Hayflick's discovery of human fibroblasts finite proliferative capacity (replicative life-span) [25] these cells have been extensively used to assess cell proliferation and senescence. Thus, we decided to explore the fatty acid synthesis pathway in early passage human primary fibroblasts exposed to DNA damaging agents capable of inducing an arrest in proliferation and senescence.

We incubated early passage human fibroblasts with doxorubicin, a topoisomerase II stabilizing drug that induces DNA double strand brakes and ROS formation leading to the activation of the DDR [6]. Doxorubicin promoted the phosphorylation and activation of the DDR sensor ATM, which in turn catalyzed the phosphorylation of p53 in Ser15 leading to increased levels of p53 and p21 and hypophosphorylation of pRb (Fig. 1A). An increase in γ-H2AX nuclear foci could also be detected in the culture soon after the treatment (Fig. 1B). Twenty-four hours after exposure to doxorubicin cell proliferation had ceased, as confirmed by the decrease in incorporation of the thymidine analogue BrdU into DNA (Fig. 1C). Induction of senescence by doxorubicin was further confirmed by the late appearance of SA-β-Gal positive cells, which were 90 ± 2 % of the culture fifteen days after exposure to the drug (Fig. 1D).

We then looked at ACC1, the enzyme that catalyzes the rate-limiting step in fatty-acid biosynthesis. In addition to the activation of the DDR doxorubicin produced an immediate decrease in ACC1 protein levels that paralleled ATM phosphorylation (Fig. 1A). After twenty-four hours of incubation with the drug a significant drop in ACC1 protein levels was observed (Fig. 1E); that correlated with a reduction in ACC1 mRNA levels (Fig. 1F), suggesting that ACC1 down-regulation might occur at least in part at the transcriptional level.

Fatty acids are a major constituent of cell lipids, forming part of phospholipids, triglycerides and cholesterol esters. We evaluated the impact of ACC1 down-regulation on endogenous lipid synthesis measuring the incorporation of the 2-^{14}C labeled acetate into cellular lipids obtained by extraction with organic solvents. A decrease in lipid synthesis was observed in doxorubicin treated cells in agreement with the drop in ACC1 levels (Fig. 1G).

We then explored if other DNA damaging agents could impact on lipid synthesis in human fibroblasts. Hydrogen peroxide (H_2O_2), an oxidant formed in biological systems, can produce DNA damage through the formation of high oxidant species like hydroxyl radical [26]. Exposure of human fibroblasts to two rounds of H_2O_2 (600 μM) spaced over an interval of five days activated the DDR and induced premature senescence. Phosphorylation of ATM and p53, along with increased p53 and p21 levels; hypophosphorylation of pRb and γ-H2AX nuclear foci could be detected in the culture twenty-four hours after the second exposure to the oxidant (Fig. 2A and B). Cell proliferation, measured by incorporation of BrdU into DNA, sharply decreased twenty-four hours after exposure to the oxidant and was still arrested seven days after (Fig. 2C). SA-β-Gal positive cells became significantly higher seven days after the second incubation with H_2O_2, with more than one-half of the culture presenting positive staining (Fig. 2D).

In agreement with our observations in doxorubicin treated cells, activation of the DDR and proliferation arrest in cells exposed to H_2O_2 were accompanied by a decrease in ACC1 protein (Fig. 2A and E) and mRNA levels (Fig. 2F) and by an inhibition of endogenous lipid synthesis in the culture (Fig. 2G). Our results suggest that DNA damaging agents produce a coordinate inhibition of proliferation and fatty acid synthesis.

3.2. Inhibition of lipid synthesis in replicative senescence

To study fatty acid metabolism in replicative senescence we obtained human fibroblasts with different cumulative population doublings (cPD) by sub cultivating early passage cells (Fig. 3A). As the cPD increased, the percentage of SA-β-Gal positive cells in the culture increased, becoming approximately 80% of the culture when proliferation had totally ceased (Fig. 3B). A decline in lipid synthesis was observed as the cPD of the culture increased, which paralleled the appearance of SA-β-Gal positive cells in the culture (Fig. 3B). This decline correlated with a reduction in the protein (Fig. 3C and D) and mRNA levels of ACC1 (Fig. 3E) in senescent cells with respect to early passage cells. A decrease in protein levels of FAS was also observed in replicative senescent cells (Fig. 3C and F), but it was not accompanied by a decrease in mRNA, that were 2 ± 0.1 fold higher than control levels (n=6, $P<0.001$).

3.3. Inhibition of lipid synthesis quiescent human fibroblasts

To test if inhibition of fatty acid synthesis was specific of senescent cells, or could be found in other proliferation-arrested cells, we measured ACC1 levels in quiescent human fibroblast. Fibroblasts were incubated in media with 0.1% serum for three days [27] and in these conditions the DDR was not activated, but pRb was hypophosphorylated (Fig. S1A) and cell proliferation was greatly reduced (Fig. S1B). Quiescent cells presented low ACC1 protein levels when compared with control cells, treated in complete media with 10% serum (Fig. S1A and C). In fact, ACC1 protein levels in quiescent fibroblasts were comparable to those of doxorubicin treated fibroblasts (Fig. S1A and C), suggesting that decreased ACC1 is not specific of senescent cells but rather characteristic of growth-arrested cells. However, ACC1 mRNA levels in quiescent cells did not accompany the decrease in protein levels, and were more than two-fold higher than those of control cells (Fig. S1D), implying the existence post-transcriptional or post-translational regulation of ACC1 in these conditions.

3.4. ShRNA targeting of ACC1 induces a senescent-like arrest in proliferation in human primary fibroblasts

Since our results showed a correlation between ACC1 levels, lipid synthesis and proliferation; we decided to evaluate the effect of inhibiting lipid synthesis on proliferating human fibroblasts. We obtained a stable knockdown of ACC1 in human fibroblasts by transduction with lentiviral particles carrying shRNA targeting ACC1 or control plasmids and selecting with puromycin. ShRNA targeting ACC1 markedly reduced the protein levels of the enzyme (Fig. 4A), and a significant decrease in endogenous lipid synthesis was observed when compared with cells transduced with control plasmids (Fig. 4B).

ACC1 shRNA targeting strongly affected cell proliferation. The incorporation of [methyl-^{3}H] thymidine into DNA, normalized to total cell protein, was significantly reduced (Fig. 4C), as was the percentage of cell nuclei that incorporated BrdU (Fig. 4D). Since arrest in proliferation is often accompanied by the induction of senescence in human fibroblasts exposed to stress, we measured several markers associated with this state. ShRNA ACC1 treated cells presented persistent activation of the DDR: a two-fold increase in the phosphorylation of ATM and a three-fold increase in the phosphorylation its substrate H2AX on Ser139 was observed (Fig. 4E), along with appearance of γ-H2AX nuclear foci

(Fig. 4F). ACC1 shRNA targeting did not increase the levels of p53 and p21; but a small and significant 21% increase in p16 along with hypophosphorylation of pRb was observed (Fig. 4E). Besides, a nearly three-fold increase in SA-β-Gal positive cells was observed after silencing of ACC1 gene expression (Fig. 4G).

To confirm that senescence induction was not due to an off-target effect of the shRNA construct, we silenced ACC1 gene expression using different shRNAs (ACC1_#2) (Fig. S2A) or treated ACC1 with the pharmacological inhibitor TOFA at a concentration that effectively inhibits lipid synthesis (Fig. S2D). Both experimental approaches resulted in a two to three-fold increase in SA-β-Gal positivity (Fig. S2C and F), supporting inhibition of fatty acid synthesis as a trigger of a senescent like response. We also performed controls with a shRNA construct containing a sequence that does not target any known human gene, but engages the RNA-induced silencing complex (RISC). This non-targeting control (NT) did not increase SA-β-Gal staining in relation to the control (Fig. S2C).

3.5. Reactive oxygen species activate the DDR and p38 MAPK in ACC1 shRNA treated cells, contributing to the establishment of the senescent phenotype

To further understand the mechanisms involved in the establishment of the senescent phenotype in ACC1 depleted cells, we measured oxidant levels and activation of p38 MAPK. Increased ROS and p38 MAPK activation are considered a major determinant of the senescent program and treatments aimed to protect the cell from oxidant species or to inhibit p38 MAPK, prevent or delay the onset of senescence [28].

We measured p38 MAPK activation assessing its phosphorylation on Thr180 and Tyr182 by upstream mitogen activated protein kinase kinases (MAPKKs) [29]. p38 MAPK phosphorylation was stimulated by ACC1 silencing, while the overall expression of the kinase was not affected (Fig. 5A). As such, the ratio between the phosphorylated enzyme and total enzyme was more than three-fold higher in ACC1 shRNA treated cells than in the control (Fig. 5A).

Intracellular ROS were assessed, measuring the oxidation of a derivative of DCFH to the fluorescent compound DCF [24]. Intracellular DCF fluorescence was increased in ACC1 shRNA treated cells in comparison with control cells, and incubation with *N*-acetylcysteine (NAC), an antioxidant that serves as precursor of intracellular cysteine and glutathione [30], reduced DCF fluorescence to similar levels in control cells and in those lacking ACC1 (Fig. 5B).

Since previous reports informed that p38 MAPK was activated by oxidants [31] we measured p38 MAPK phosphorylation in cells incubated with NAC. Incubation with the antioxidant decreased the phosphorylation of p38 MAPK in shACC1 treated cells (Fig. 5C, Fig. S3A); suggesting that oxidant species are involved in p38 MAPK activation in this setting. N-acetylcysteine treatment also reduced H2AX phosphorylation in shACC1 cells (Fig. 5D, Fig. S3B) and reduced the percentage of cells staining positive for SA-β-Gal (Fig. 5E) in shACC1 treated cells. These results are in agreement with previous reports on oxidant species involvement in the activation of the DDR pathway [32, 33] and induction of senescence [34]. However, incubation with the antioxidant did not rescue the shACC1

treated cells from proliferation arrest, measured as [methyl-^{3}H] thymidine incorporation to DNA (Fig. S4A), nor could it restore pRb phosphorylation (Fig. S4B).

We then explored the effects of the p38 MAPK inhibitor SB203580 on the induction of senescence in shACC1 treated cells. Similar to NAC, pharmacological inhibition of p38 MAPK reduced SA-β-Gal staining (Fig. 5E), but did not restore proliferation (not shown). Together, these results implicate ROS and p38 MAPK in certain aspects of the senescent program induced by inhibition of lipid synthesis in human fibroblasts.

3.6. ShRNA targeting and pharmacological inhibitors of FAS induce a senescent-like arrest in proliferation in human primary fibroblasts

To assess if the results obtained were specific for ACC1 silencing or more generally related to the inhibition of fatty acid synthesis, we next silenced the expression of the fatty acid synthase (FAS) gene. Transduction of early human fibroblasts with lentiviral particles carrying shRNA targeting FAS substantially reduced FAS protein levels (Fig. 6A) and inhibited endogenous lipid synthesis (Fig. 6B).

As observed for ACC1 gene silencing, shFAS treatment inhibited cell proliferation measured as the incorporation of [methyl-^{3}H] thymidine into DNA per mg of protein (Fig. 6C) and increased SA-β-Gal staining (Fig. 6D). Activation of the DDR was also observed, since shRNA FAS treated cells presented an increase in γ-H2AX levels and nuclear foci (Fig. 6E and 6F) and pRb hypophosphorylation (Fig. 6F), p38 MAPK phosphorylation was also increased in shRNA FAS treated cells (Fig. 6G).

FAS gene silencing with a second shRNA construct (FAS_#2) (Fig. S2B) or treatment with FAS pharmacological inhibitor C75 [35], at a concentration that inhibits lipid synthesis to 32 ± 2% of control (Fig. S2E), increased SA-β-Gal staining two to three-fold over control levels (Fig. S2C and F), further supporting fatty acid synthesis inhibition as a trigger of cellular senescence.

4. Discussion

Cell proliferation requires an active anabolism in order to provide building blocks for the new cells, and several lines of evidence point to a coordinate regulation between proliferation and metabolism [8]. Furthermore, the influence of metabolism on the cell phenotype appears to transcend proliferation, impacting as well on cell function [36].

Existing evidence supports that metabolic changes accompany cell fate decisions and phenotypic alterations. However few studies have addressed the fatty acid synthesis pathway in senescent cells. Maeda et al. observed that FAS and stearoyl-CoA desaturase-1 levels were decreased in replicative senescent fibroblasts, affecting membrane lipid composition [16]. Our results expand their observations to ACC1 levels and identify inhibition of the fatty acid synthesis pathway as a common characteristic of cells undergoing both replicative and premature senescence, as well as quiescence-triggered proliferation arrest. It is worth noting that fibroblasts undergoing HRAS^{G12V} oncogene induced senescence, also demonstrate an inhibition of endogenous lipid synthesis, but due to ACC1 inhibition by

phosphorylation [14]. All together our results support a coordinate regulation of the fatty acid synthesis enzymes with proliferation requirements in human fibroblasts. Similar observations have been reported for other anabolic routes were tumor suppressor p53 regulates the level and activity of the malic enzymes [37] and glucose-6-phosphate dehydrogenase [38]. Moreover, in adipocytes p53 has been shown to suppress the expression of SBREP1c, FAS and ATP citrate lyase, inhibiting lipid synthesis [39], and is a likely candidate to control ACC1 expression in senescent cells.

Cyclin D1 the regulatory subunit of the holoenzyme cyclin D1/cyclin dependent kinase that phosphorylates and inactivates pRB negatively regulates the expression of the lipogenic enzymes ACC1 and FAS in mouse mammary epithelium [13]. Since cyclin D1 levels are increased in senescent fibroblasts [40], this pathway could also be responsible for the decrease in expression of ACC1 in replicative and premature senescence.

Other lines of investigation point toward the anaphase promoting complex/cyclosome (APC/C) as a common regulator of both the G1 to S phase transition and the levels of key enzymes involved in glycolysis and glutaminolysis [41, 42]. APC/C is a ubiquitin ligase complex that binds to its ligands and targets them for proteasomal degradation through their degradation motifs, the D box and KEN box [43]. Interestingly, ACC1 possesses a KEN box making it a possible candidate for APC/C mediated proteasomal degradation.

We reasoned that if proliferation and lipid synthesis were tightly linked, disruption of this metabolic pathway would have a negative impact on proliferating cells. Previous reports have shown that pharmacological inhibition or silencing of ACC1 or FAS gene expression inhibits cell proliferation and leads to apoptosis in cancer cell lines but not in non-malignant cells, and argued in favor of a selective toxic action towards cancer cells [9]. Our data showed that silencing of the fatty acid synthesis enzymes ACC1 and FAS led to a decrease in DNA synthesis and the appearance of several markers of cell senescence in human fibroblasts. Although p53 and p21 levels were not augmented, a small but significant increase in the levels of the cyclin-dependent kinase inhibitor p16 could be observed; that could be responsible for the decrease in pRb phosphorylation in this setting.

Reactive oxygen species were increased in ACC1 depleted senescent cells, and activation of the DDR and increase in SA-β-Gal were inhibited by the addition of the antioxidant NAC. However, incubation with NAC failed to restore proliferation and to revert pRb hypophosphorylated status, suggesting that the increase in ROS is not the only determinant in the establishment of cell senescence and proliferation arrest. Although the source of oxidant species was not explored, mitochondria appear as likely candidates in this setting, since absence of ACC1 could result in an increase in fatty acid oxidation and concomitantly mitochondrial superoxide formation [44]. A decrease in endogenous fatty acid synthesis could also affect phospholipid and mitochondrial membrane composition, impacting on the formation of superoxide by the mitochondrial complexes [45, 46].

Further analysis led us to uncover a role for p38 MAPK in the induction of senescence by inhibition of lipid synthesis, since increased phosphorylation of p38 was observed upon ACC1 and FAS shRNA targeting and addition of a pharmacological inhibitor of this kinase

resulted in decreased SA-β-Gal staining in ACC1 depleted fibroblasts. We further identified reactive oxygen species as activators of p38 MAPK in this setting; since incubation with NAC reduced p38 MAPK phosphorylation.

5. Conclusions

Overall our results support the existence of a tight coordination between the fatty acid synthesis pathway and cell proliferation in human fibroblasts. In particular, levels of the rate-limiting enzyme in the fatty acid synthesis pathway, ACC1, are significantly diminished in human fibroblast undergoing both senescence and quiescence proliferation arrests. Concordantly endogenous lipid synthesis is reduced as fibroblasts cease their proliferation, and their requirement for biosynthetic precursors drops.

Furthermore, our findings demonstrate that inhibition of lipid synthesis in proliferating fibroblasts leads to growth arrest and the appearance of several markers of senescence. Our results, in combination with other reports [37, 47] support metabolic alterations as a new trigger for senescence.

Supplementary Material

Refer to Web version on PubMed Central for supplementary material.

Acknowledgements

We would like to thank Dr. Rafael Radi for the critical revision of the manuscript, Dr. Mercedes Rodríguez-Teja for her help in molecular biology assays and Paola Rosenberg for technical assistance.

Funding information

This work was supported by NIH Intramural funds awarded to TF; Fondo Clemente Estable-ANII (FCE_6381) and CSIC I+D 2012 (ID 47) and Programa de Desarrollo de las Ciencias Básicas (PEDECIBA) to CQ; Espacio Interdisciplinario Centros, UDELAR 2015 to CQ, LC and AT; CSIC grupos I+D 2014 (767) to LC; CSIC grupos I +D 2014 (563) to AT and CSIC Iniciación to IM and JM. IM and JM have scholarships from the ANII.

Abbreviations

ACC1	acetyl-CoA carboxylase 1
ATM	Ataxia Telangiectasia Mutated kinase
BrdU	bromodeoxyuridine
CM-DCFHDA	5(and-6)-chloromethyl-2′,7′-dichlorodihydrofluorescein diacetate
DCF	2’-7’-dichlorofluorescein
DCFH	2’-7’-dichlorodihydrofluorescein
DDR	DNA damage response
Cdk	cyclin dependent kinase
cPD	cumulative population doubling level

FAS	fatty acid synthase
H_2O_2	hydrogen peroxide
NAC	N-acetylcysteine
PDL	population doubling level
p38 MAPK	p38 mitogen activated protein kinase
ROS	reactive oxygen species
pRb	Retinoblastoma protein
SA-β-Gal	senescence associated β-galactosidase activity
shRNA	short hairpin ribonucleic acid

References

1. Munoz-Espin D, Serrano M. Cellular senescence: from physiology to pathology. Nature reviews. Molecular cell biology. 2014; 15:482–496. [PubMed: 24954210]
2. Campisi J. Aging, cellular senescence, and cancer. Annu Rev Physiol. 2013; 75:685–705. [PubMed: 23140366]
3. d'Adda di Fagagna F. Living on a break: cellular senescence as a DNA-damage response. Nature reviews. Cancer. 2008; 8:512–522. [PubMed: 18574463]
4. Passos JF, Nelson G, Wang C, Richter T, Simillion C, Proctor CJ, Miwa S, Olijslagers S, Hallinan J, Wipat A, Saretzki G, Rudolph KL, Kirkwood TB, von Zglinicki T. Feedback between p21 and reactive oxygen production is necessary for cell senescence. Molecular systems biology. 2010; 6:347. [PubMed: 20160708]
5. Barascu A, Le Chalony C, Pennarun G, Genet D, Imam N, Lopez B, Bertrand P. Oxidative stress induces an ATM-independent senescence pathway through p38 MAPK-mediated lamin B1 accumulation. The EMBO journal. 2012; 31:1080–1094. [PubMed: 22246186]
6. Kurz EU, Douglas P, Lees-Miller SP. Doxorubicin activates ATM-dependent phosphorylation of multiple downstream targets in part through the generation of reactive oxygen species. J Biol Chem. 2004; 279:53272–53281. [PubMed: 15489221]
7. Perez-Mancera PA, Young AR, Narita M. Inside and out: the activities of senescence in cancer. Nature reviews. Cancer. 2014; 14:547–558. [PubMed: 25030953]
8. Ward PS, Thompson CB. Metabolic reprogramming: a cancer hallmark even warburg did not anticipate. Cancer Cell. 2012; 21:297–308. [PubMed: 22439925]
9. Menendez JA, Lupu R. Fatty acid synthase and the lipogenic phenotype in cancer pathogenesis. Nature reviews. Cancer. 2007; 7:763–777. [PubMed: 17882277]
10. Abu-Elheiga L, Almarza-Ortega DB, Baldini A, Wakil SJ. Human acetyl-CoA carboxylase 2. Molecular cloning, characterization, chromosomal mapping, and evidence for two isoforms. J Biol Chem. 1997; 272:10669–10677. [PubMed: 9099716]
11. Tong L. Acetyl-coenzyme A carboxylase: crucial metabolic enzyme and attractive target for drug discovery. Cell Mol Life Sci. 2005; 62:1784–1803. [PubMed: 15968460]
12. Ray H, Suau F, Vincent A, Dalla Venezia N. Cell cycle regulation of the BRCA1/acetyl-CoA-carboxylase complex. Biochem Biophys Res Commun. 2009; 378:615–619. [PubMed: 19061860]
13. Sakamaki T, Casimiro MC, Ju X, Quong AA, Katiyar S, Liu M, Jiao X, Li A, Zhang X, Lu Y, Wang C, Byers S, Nicholson R, Link T, Shemluck M, Yang J, Fricke ST, Novikoff PM, Papanikolaou A, Arnold A, Albanese C, Pestell R. Cyclin D1 determines mitochondrial function in vivo. Mol Cell Biol. 2006; 26:5449–5469. [PubMed: 16809779]

14. Quijano C, Cao L, Fergusson MM, Romero H, Liu J, Gutkind S, Rovira II, Mohney RP, Karoly ED, Finkel T. Oncogene-induced senescence results in marked metabolic and bioenergetic alterations. Cell Cycle. 2012; 11:1383–1392. [PubMed: 22421146]
15. Kim YM, Shin HT, Seo YH, Byun HO, Yoon SH, Lee IK, Hyun DH, Chung HY, Yoon G. Sterol regulatory element-binding protein (SREBP)-1-mediated lipogenesis is involved in cell senescence. J Biol Chem. 2010; 285:29069–29077. [PubMed: 20615871]
16. Maeda M, Scaglia N, Igal RA. Regulation of fatty acid synthesis and Delta9-desaturation in senescence of human fibroblasts. Life Sci. 2009; 84:119–124. [PubMed: 19059270]
17. Chen JH, Stoeber K, Kingsbury S, Ozanne SE, Williams GH, Hales CN. Loss of proliferative capacity and induction of senescence in oxidatively stressed human fibroblasts. J Biol Chem. 2004; 279:49439–49446. [PubMed: 15377661]
18. Howard BV, Howard WJ, Bailey JM. Acetyl coenzyme A synthetase and the regulation of lipid synthesis from acetate in cultured cells. J Biol Chem. 1974; 249:7912–7921. [PubMed: 4473453]
19. Bligh EG, Dyer WJ. A rapid method of total lipid extraction and purification. Can J Biochem Physiol. 1959; 37:911–917. [PubMed: 13671378]
20. Dimri GP, Lee X, Basile G, Acosta M, Scott G, Roskelley C, Medrano EE, Linskens M, Rubelj I, Pereira-Smith O, et al. A biomarker that identifies senescent human cells in culture and in aging skin in vivo. Proc Natl Acad Sci U S A. 1995; 92:9363–9367. [PubMed: 7568133]
21. Livak KJ, Schmittgen TD. Analysis of relative gene expression data using real-time quantitative PCR and the 2(-Delta Delta C(T)) Method. Methods. 2001; 25:402–408. [PubMed: 11846609]
22. Cristofalo, VJ.; Volker, C.; Allen, RG. Use of the Fibroblast Model in the Study of Cellular Senescence. In: Barnett, Y.A.B.a.C.R., editor. Methods in Molecular Medicine: Aging Methods and Protocols. Humana Press Inc.; 2000. p. 23-52.Place Published
23. Goncharova EA, Lim P, Goncharov DA, Eszterhas A, Panettieri RA Jr. Krymskaya VP. Assays for in vitro monitoring of proliferation of human airway smooth muscle (ASM) and human pulmonary arterial vascular smooth muscle (VSM) cells. Nature protocols. 2006; 1:2905–2908. [PubMed: 17406550]
24. Halliwell, B.; Gutteridge, JMC. Measurement of Reactive Species, Free radicals in Biology and Medicine. Oxford University Press; 2015. p. 284-353.Place Published
25. Hayflick L. The Limited in Vitro Lifetime of Human Diploid Cell Strains. Exp Cell Res. 1965; 37:614–636. [PubMed: 14315085]
26. Mello Filho AC, Hoffmann ME, Meneghini R. Cell killing and DNA damage by hydrogen peroxide are mediated by intracellular iron. The Biochemical journal. 1984; 218:273–275. [PubMed: 6712613]
27. Lemons JM, Feng XJ, Bennett BD, Legesse-Miller A, Johnson EL, Raitman I, Pollina EA, Rabitz HA, Rabinowitz JD, Coller HA. Quiescent fibroblasts exhibit high metabolic activity. PLoS Biol. 2010; 8:e1000514. [PubMed: 21049082]
28. Borodkina A, Shatrova A, Abushik P, Nikolsky N, Burova E. Interaction between ROS dependent DNA damage, mitochondria and p38 MAPK underlies senescence of human adult stem cells. Aging. 2014; 6:481–495. [PubMed: 24934860]
29. Cargnello M, Roux PP. Activation and function of the MAPKs and their substrates, the MAPK-activated protein kinases. Microbiol Mol Biol Rev. 2011; 75:50–83. [PubMed: 21372320]
30. Rushworth GF, Megson IL. Existing and potential therapeutic uses for N-acetylcysteine: the need for conversion to intracellular glutathione for antioxidant benefits. Pharmacol Ther. 2014; 141:150–159. [PubMed: 24080471]
31. Ito K, Hirao A, Arai F, Takubo K, Matsuoka S, Miyamoto K, Ohmura M, Naka K, Hosokawa K, Ikeda Y, Suda T. Reactive oxygen species act through p38 MAPK to limit the lifespan of hematopoietic stem cells. Nat Med. 2006; 12:446–451. [PubMed: 16565722]
32. Liu J, Cao L, Chen J, Song S, Lee IH, Quijano C, Liu H, Keyvanfar K, Chen H, Cao LY, Ahn BH, Kumar NG, Rovira II, Xu XL, van Lohuizen M, Motoyama N, Deng CX, Finkel T. Bmi1 regulates mitochondrial function and the DNA damage response pathway. Nature. 2009; 459:387–392. [PubMed: 19404261]

33. Zhao H, Traganos F, Albino AP, Darzynkiewicz Z. Oxidative stress induces cell cycle-dependent Mre11 recruitment, ATM and Chk2 activation and histone H2AX phosphorylation. Cell Cycle. 2008; 7:1490–1495. [PubMed: 18418078]
34. Lee AC, Fenster BE, Ito H, Takeda K, Bae NS, Hirai T, Yu ZX, Ferrans VJ, Howard BH, Finkel T. Ras proteins induce senescence by altering the intracellular levels of reactive oxygen species. J Biol Chem. 1999; 274:7936–7940. [PubMed: 10075689]
35. Kuhajda FP, Pizer ES, Li JN, Mani NS, Frehywot GL, Townsend CA. Synthesis and antitumor activity of an inhibitor of fatty acid synthase. Proc Natl Acad Sci U S A. 2000; 97:3450–3454. [PubMed: 10716717]
36. MacIver NJ, Michalek RD, Rathmell JC. Metabolic regulation of T lymphocytes. Annu Rev Immunol. 2013; 31:259–283. [PubMed: 23298210]
37. Jiang P, Du W, Mancuso A, Wellen KE, Yang X. Reciprocal regulation of p53 and malic enzymes modulates metabolism and senescence. Nature. 2013; 493:689–693. [PubMed: 23334421]
38. Jiang P, Du W, Wang X, Mancuso A, Gao X, Wu M, Yang X. p53 regulates biosynthesis through direct inactivation of glucose-6-phosphate dehydrogenase. Nat Cell Biol. 2011; 13:310–316. [PubMed: 21336310]
39. Goldstein I, Rotter V. Regulation of lipid metabolism by p53 - fighting two villains with one sword. Trends in endocrinology and metabolism: TEM. 2012; 23:567–575. [PubMed: 22819212]
40. Dulic V, Drullinger LF, Lees E, Reed SI, Stein GH. Altered regulation of G1 cyclins in senescent human diploid fibroblasts: accumulation of inactive cyclin E-Cdk2 and cyclin D1-Cdk2 complexes. Proc Natl Acad Sci U S A. 1993; 90:11034–11038. [PubMed: 8248208]
41. Almeida A, Bolanos JP, Moncada S. E3 ubiquitin ligase APC/C-Cdh1 accounts for the Warburg effect by linking glycolysis to cell proliferation. Proc Natl Acad Sci U S A. 2010; 107:738–741. [PubMed: 20080744]
42. Colombo SL, Palacios-Callender M, Frakich N, De Leon J, Schmitt CA, Boorn L, Davis N, Moncada S. Anaphase-promoting complex/cyclosome-Cdh1 coordinates glycolysis and glutaminolysis with transition to S phase in human T lymphocytes. Proc Natl Acad Sci U S A. 2010; 107:18868–18873. [PubMed: 20921411]
43. Moncada S, Higgs EA, Colombo SL. Fulfilling the metabolic requirements for cell proliferation. The Biochemical journal. 2012; 446:1–7. [PubMed: 22835215]
44. Kakimoto PA, Tamaki FK, Cardoso AR, Marana SR, Kowaltowski AJ. H2O2 release from the very long chain acyl-CoA dehydrogenase. Redox Biol. 2015; 4:375–380. [PubMed: 25728796]
45. Rossato FA, Zecchin KG, La Guardia PG, Ortega RM, Alberici LC, Costa RA, Catharino RR, Graner E, Castilho RF, Vercesi AE. Fatty acid synthase inhibitors induce apoptosis in non-tumorigenic melan-a cells associated with inhibition of mitochondrial respiration. PLoS One. 2014; 9:e101060. [PubMed: 24964211]
46. Schenkel LC, Bakovic M. Formation and regulation of mitochondrial membranes. Int J Cell Biol. 2014; 2014:709828. [PubMed: 24578708]
47. Jones RG, Plas DR, Kubek S, Buzzai M, Mu J, Xu Y, Birnbaum MJ, Thompson CB. AMP-activated protein kinase induces a p53-dependent metabolic checkpoint. Mol Cell. 2005; 18:283–293. [PubMed: 15866171]
48. Stewart SA, Dykxhoorn DM, Palliser D, Mizuno H, Yu EY, An DS, Sabatini DM, Chen IS, Hahn WC, Sharp PA, Weinberg RA, Novina CD. Lentivirus-delivered stable gene silencing by RNAi in primary cells. RNA. 2003; 9:493e501. [PubMed: 12649500]

Highlights

- ACC1 protein and mRNA level are decreased in premature and replicative senescence.
- Lipid synthesis decreases in premature and replicative senescence.
- Inhibition of ACC1 or FAS induces proliferation arrest and markers of senescence.
- ACC1 deletion increases oxidant levels leading to p38 MAPK and DDR activation.

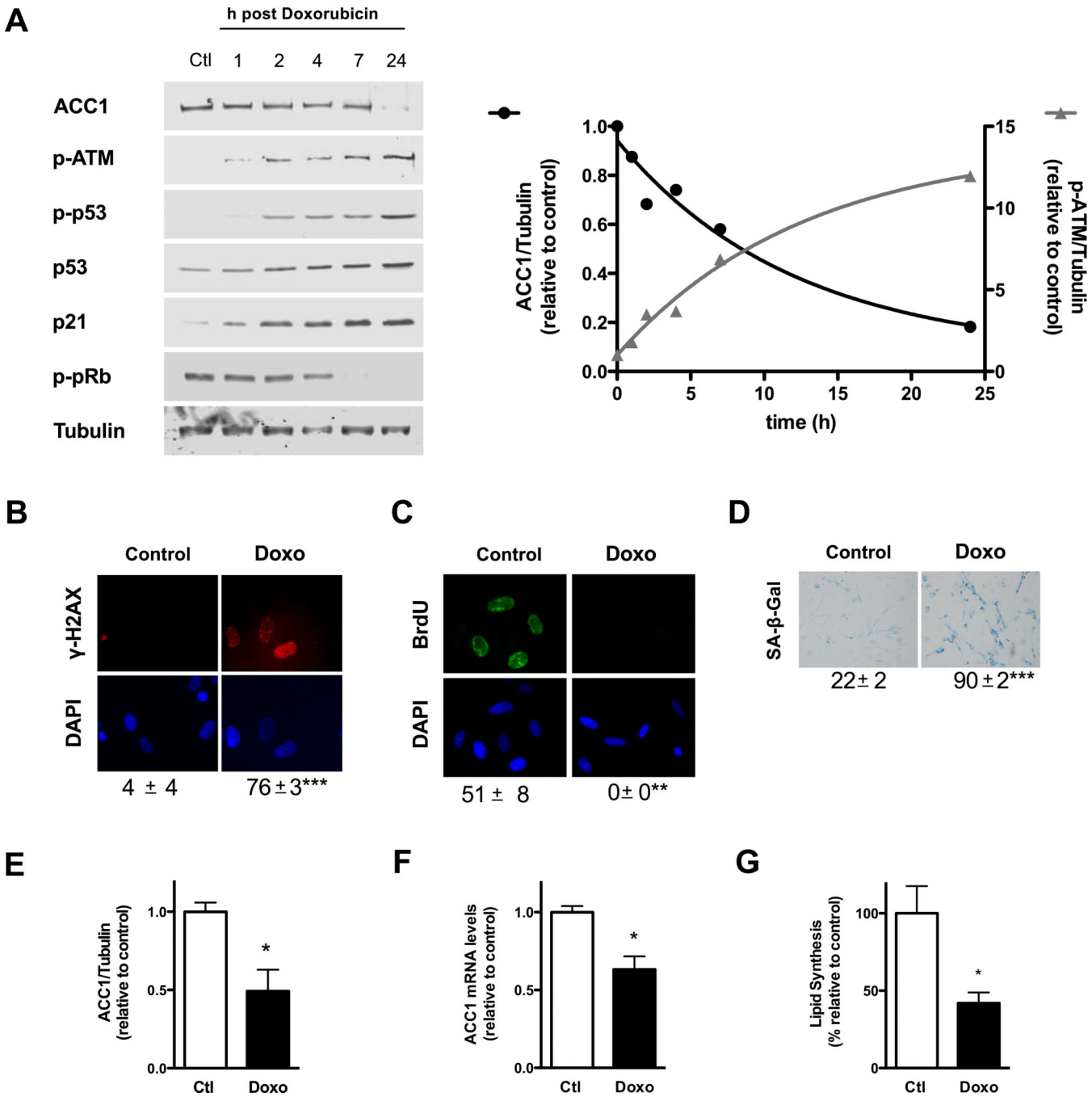

Figure 1. ACC1 levels, expression and lipid synthesis decrease immediately after the exposure to doxorubicin

Early passage human fibroblasts were exposed for twenty-four hours to either doxorubicin 0.2 μM (Doxo) or the vehicle DMSO, (Control, Ctl) in complete media. All measurements were done at the end of the treatment, unless otherwise specified. (A) ACC1 levels, ATM phosphorylation (p-ATM), p53 phosphorylation (p-p53), p53, p21 and pRb phosphorylation (p-pRB) were assessed by Western blot at different times during the incubation, tubulin was used as loading control. The graph on the right shows the data obtained after quantifying the blots and normalizing ACC1 and p-ATM levels to tubulin. Control cells were incubated with

DMSO for 24 hours. (B) γ-H2AX foci were assessed by immunofluorescence, original magnification X400. The percentage of cells with nuclear foci is shown below the picture. (C) Cell proliferation was measured by immunofluorescence, as BrdU incorporation to nuclear DNA, original magnification X400. The percentage of cells with positive nuclear staining is shown below the picture. (D) SA-β-Gal staining was assessed by light microscopy, original magnification X40, 15 days after exposure to doxorubicin. The percentage of positive cells is shown below the picture. (E) Twenty-four hours after the exposure to the drug ACC1 and tubulin levels were determined in independent Western blots and protein levels of ACC1 were normalized using tubulin as loading control. (F) ACC1 mRNA levels. (G) Lipid synthesis was determined by ^{14}C-acetate incorporation. Results are expressed as the mean ± SEM ($n \geq 3$, * $P<0.05$, ** $P<0.005$, *** $P<0.0005$).

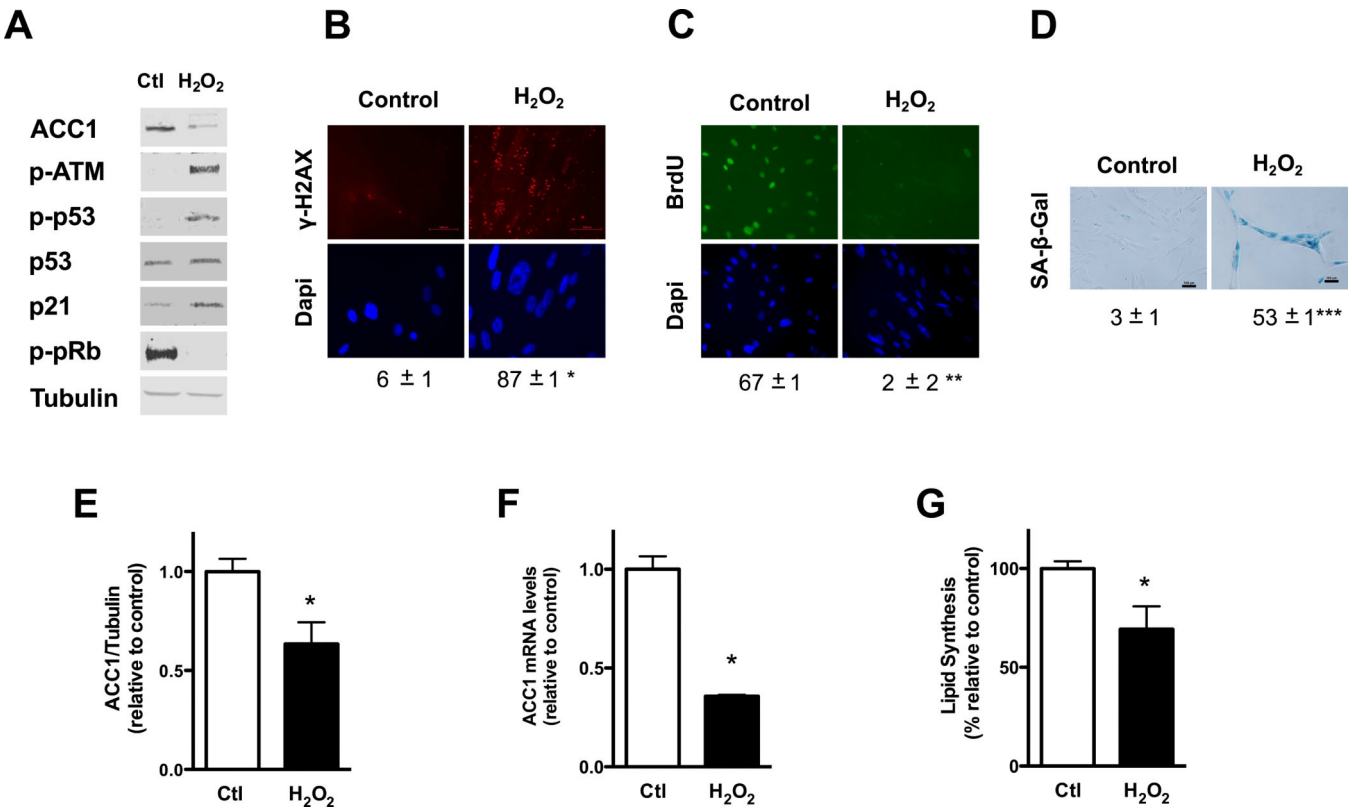

Figure 2. ACC1 protein levels, gene expression and lipid synthesis decrease after the exposure to H_2O_2

Early passage human fibroblasts were incubated with H_2O_2 in complete media (600 μM for two hours, two exposures separated by a five day interval). All measurements were done twenty-four hours after the second exposure to H_2O_2, unless otherwise specified. (A) ACC1 levels, ATM phosphorylation (p-ATM), p53 phosphorylation (p-p53), p53, p21 and pRb phosphorylation (p-pRB) were assessed by Western blot; tubulin was used as loading control. (B) γ-H2AX foci were assessed by immunofluorescence, original magnification X400. The percentage of cells with nuclear foci is shown below the picture. (C) Cell proliferation was measured by immunofluorescence as BrdU incorporation to nuclear DNA, original magnification X200. The percentage of cells with positive nuclear staining is shown below the picture. (D) SA-β-Gal staining was performed seven days after the second exposure to the oxidant, the percentage of positive cells was determined by light microscopy and is shown under the picture, original magnification X200. (E) Protein levels of ACC1 in control and treated cells, obtained after quantifying independent Western blots and normalized using tubulin as loading control. (F) ACC1 mRNA levels (G) Lipid synthesis was determined by ^{14}C-acetate incorporation. Results are expressed as the mean ± SEM ($n \geq 3$, *$P<0.05$, **$P<0.005$, ***$P<0.0005$). Representative blots of $n \geq 3$ independent experiments are shown.

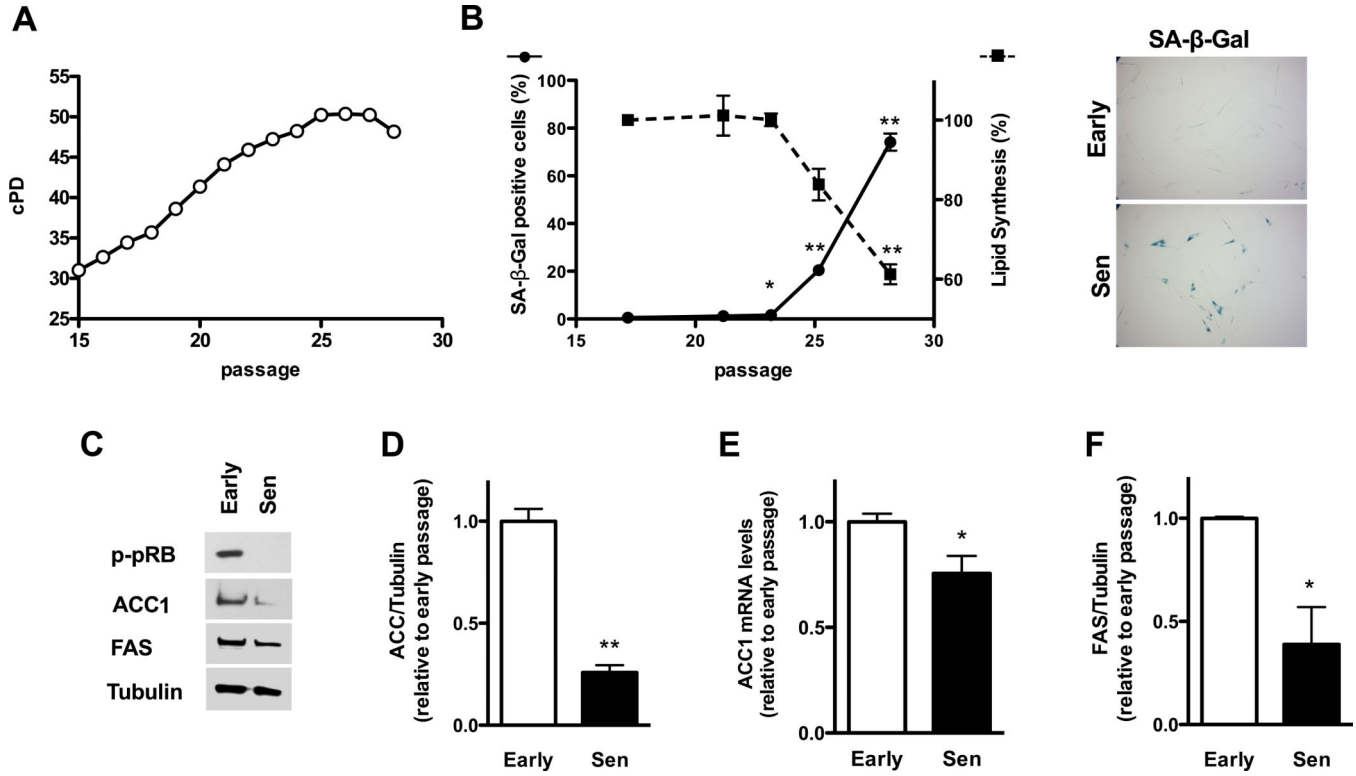

Figure 3. Lipid synthesis in replicative senescent fibroblasts

(A) Early passage human fibroblasts were expanded in culture and cumulative population doublings measured until the onset of replicative senescence (Sen). (B) Lipid synthesis and SA-β-Gal were assessed in parallel for cells with different population doublings. The pictures on the right show SA-β-Gal staining for early passage (Early) and replicative senescence (Sen) fibroblasts, original magnification X40. (C) Early passage or replicative senescent cells (Sen) were evaluated by Western blot analysis for the expression of ACC1 and FAS, and compared to a loading control protein, tubulin. (D and F) Quantification of Western blots for ACC1 and FAS are shown. (E) Shows ACC1 mRNA levels. Results are expressed as the mean ± SEM ($n \geq 3$, *$P<0.05$, **$P<0.005$).

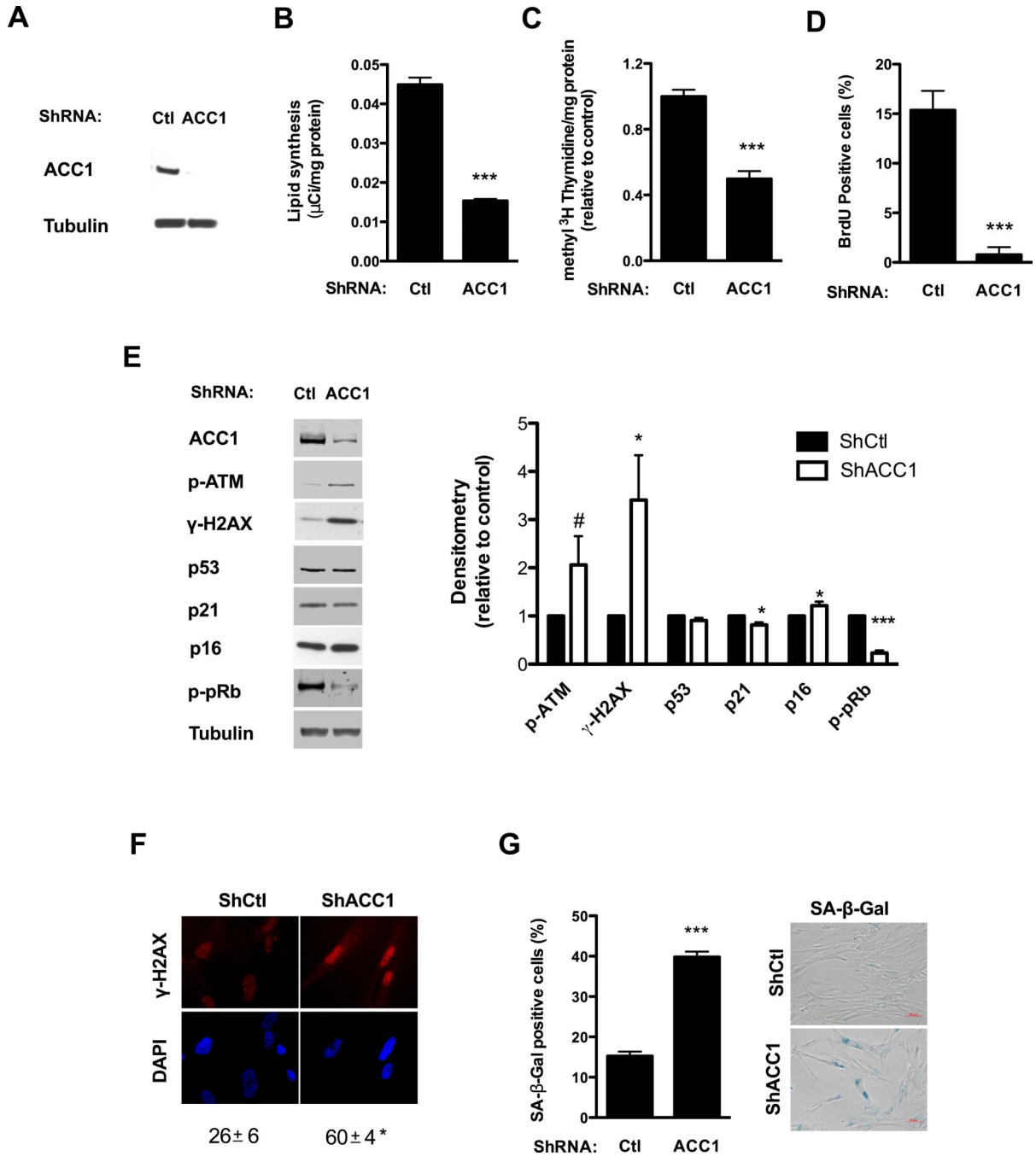

Figure 4. Knockdown of ACC1 inhibits cell proliferation and induces senescence in human fibroblasts

Early passage human fibroblasts were transduced with lentiviral particles containing either a control or ACC1 specific shRNA and subsequently selected with puromycin; assays were performed four to six days after transduction. (A) ACC1 protein levels were assessed by Western blot and (B) lipid synthesis was determined by ^{14}C-acetate incorporation. (C and D) Cell proliferation was measured as [methyl ^{3}H]-thymidine incorporation to DNA per mg of cell protein and expressed relative to control values (C); or measuring BrdU incorporation to DNA (D). (E) ATM phosphorylation (p-ATM), p53, p21, p16 and pRb phosphorylation (p-

pRB) were assessed by Western blot; tubulin was used as loading control. The graph on the right shows the protein levels of the different markers, normalized by the loading control and expressed relative to control cells. (F) γ-H2AX foci were evaluated by immunofluorescence, original magnification X400. The percentage of cells with positive nuclear foci is shown below the picture. (G) The percentage of cells with positive SA-β-Gal staining was determined by light microscopy. Representative pictures are shown on the right, original magnification X100. Results are expressed as the mean ± SEM ($n \geq 3$, #$P=0.1$, *$P<0.05$, ***$P<0.0005$). Representative blots of $n \geq 3$ independent experiments are shown.

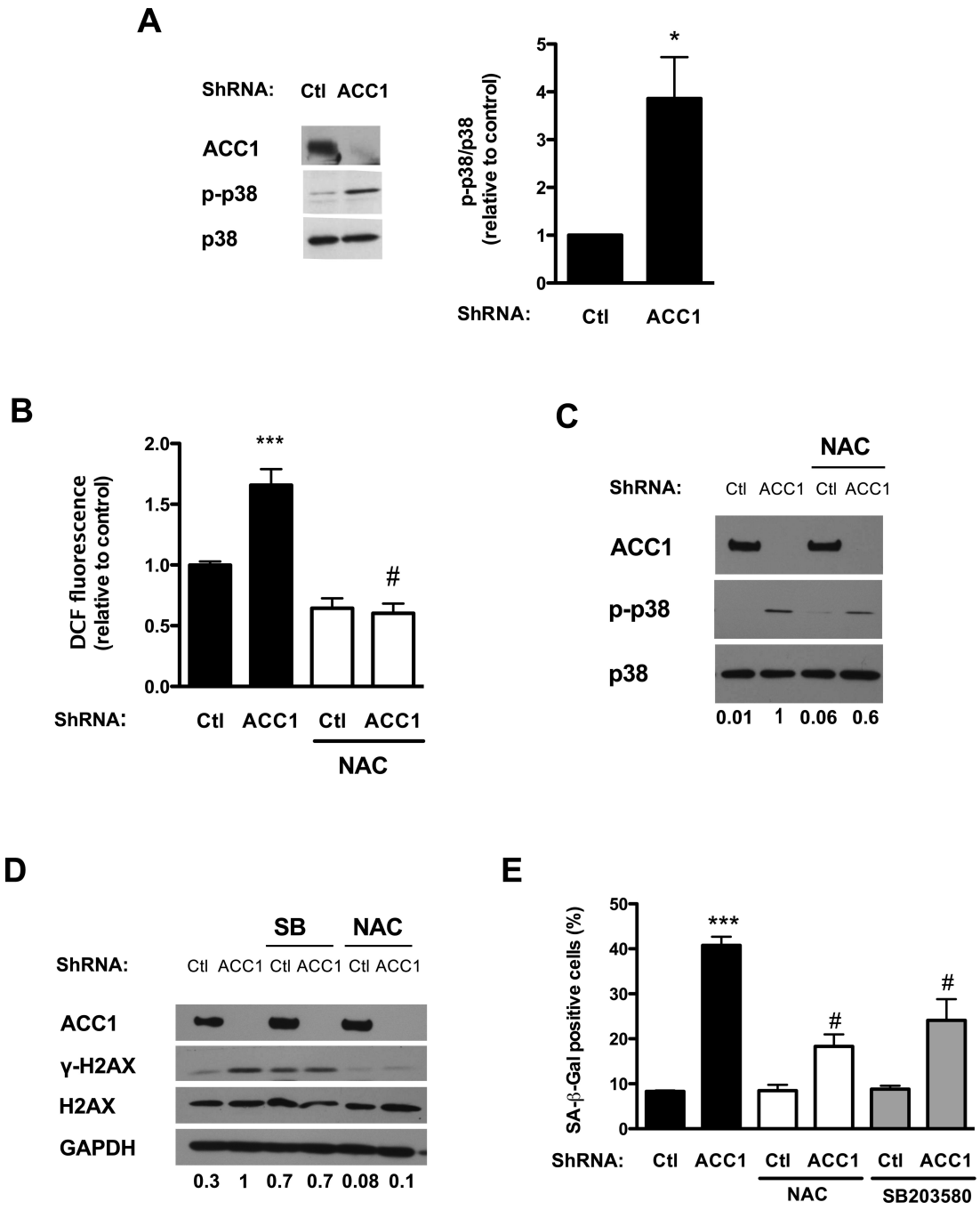

Figure 5. Reactive oxygen species and p38 MAPK play a role in the induction of senescence in ACC1 depleted cells

Early passage human fibroblasts were transduced with lentiviral particles containing either a control or an ACC1 specific shRNA. Assays were performed four to six days after transduction. (A) p38 MAPK phosphorylation (p-p38) and total p38 MAPK (p38) levels were determined by Western blot. The bands corresponding to p-p38 MAPK and p38 MAPK were quantified and the ratio between them calculated and shown in the graph on the right. A representative Western blot of n=3 independent experiments is shown. (B) Reactive oxygen species were determined measuring DCF fluorescence. Cells were incubated with 5

μM CM-DCFHDA after being treated with or without 0.75 mM N-acetylcysteine (NAC) for two hours. (C) Twenty-four hours after infection cells were switched to media supplemented with NAC (0.75 mM) or vehicle, media with NAC or vehicle was changed daily. Five days after infection, p-p38 and p38 and ACC1 levels were assessed by Western blot. The bands corresponding to p-p38 MAPK and p38 MAPK were quantified, the ratio between them calculated and expressed relative to shACC1 below the blots and in Fig. S3A. (D) Twenty-four hours after the infection the cells were switched to media with NAC (0.75 mM) or with the p38 inhibitor SB203580 (8 μM). Five days after infection γ-H2AX, total H2AX levels and ACC1 levels were assessed by Western blot. The bands corresponding to γ-H2AX were quantified and expressed relative to γ-H2AX levels in shACC1 cells below the blot and in Fig. S3B. A representative Western blot of $n=3$ independent experiments is shown. (E) SA-β-Gal positivity was determined. Results are expressed as the mean ± SEM ($n\geq3$, (*$P<0.05$, ***$P<0.0001$ Ctl vs. shACC1; #$P<0.0005$ shACC1+NAC vs. ACC1 or shACC1+SB vs. shACC1).

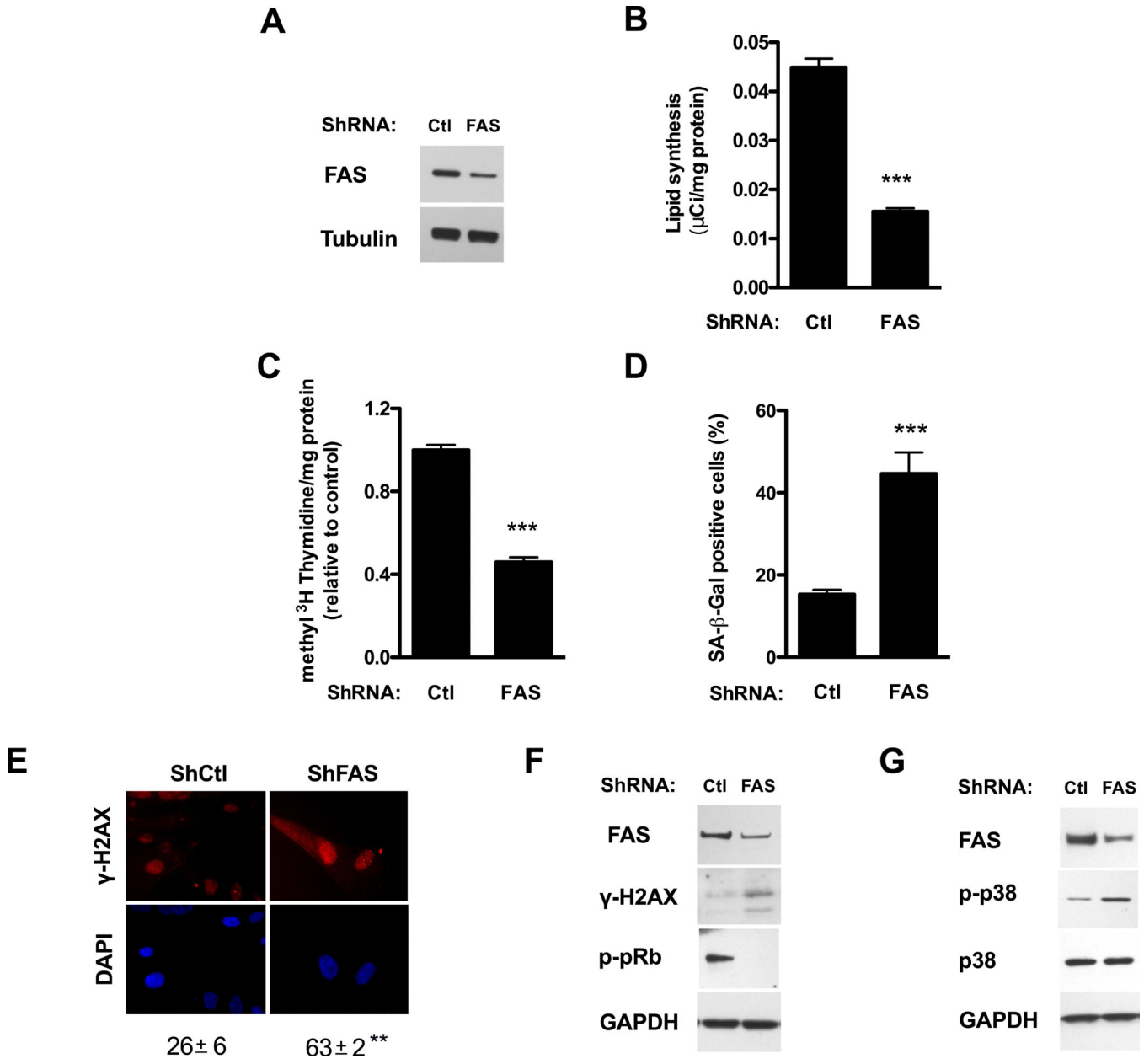

Figure 6. Knockdown of FAS inhibits lipid synthesis, reduces DNA synthesis and induces senescence

Early passage fibroblasts were transduced with lentiviral particles harboring either control or FAS specific shRNA and selected with puromycin; assays were performed four to six days after transduction. (A) Enzyme levels were assessed by Western blot. (B) Lipid synthesis was determined by ^{14}C-acetate incorporation into cell lipids. (C) Cell proliferation was measured as [methyl ^{3}H]-thymidine incorporation to DNA per mg of protein. (D) The percentage of SA-β-Gal positive cells in the culture was determined. (E) The percentage of nuclei presenting γ-H2AX foci was obtained by immunofluorescence, original magnification X400. (F) Activation of the DDR as assessed by Western blot analysis of H2AX phosphorylation (γ-H2AX) and pRb phosphorylation (p-pRb). (G) p38 MAPK level

and phosphorylation (p-p38) were assessed by Western blot. Results are expressed as the mean ± SEM ($n \geq 3$, $^{***}P < 0.0005$). Representative Western blots of $n \geq 3$ independent experiments are shown.